

1 **Theoretical insights from upscaling Michaelis-Menten microbial**
2 **dynamics in biogeochemical models: a dimensionless approach**

3
4 Chris H. Wilson¹, Stefan Gerber²

5 ¹Agronomy Department, University of Florida, Gainesville, FL, USA 32611

6 ²Soil and Water Sciences Department, University of Florida, Gainesville, FL, USA 32611

7

8 *Correspondence to:* Chris H. Wilson (chwilson@ufl.edu)

9

10

11

12

13

14

15

16

17

18

19 **Abstract.** Leading an effective response to the accelerating crisis of anthropogenic climate
20 change will require improved understanding of global carbon cycling. A critical source of
21 uncertainty in Earth Systems Models (ESMs) is the role of microbes in mediating both the
22 formation and decomposition of soil organic matter, and hence in determining patterns of CO₂
23 efflux. Traditionally, ESMs model carbon turnover as a first order process impacted primarily by
24 abiotic factors, whereas contemporary biogeochemical models often explicitly represent the
25 microbial biomass and enzyme pools as the active agents of decomposition. However, the
26 combination of non-linear microbial kinetics and ecological heterogeneity across space and time
27 guarantees that upscaled dynamics will violate mean-field assumptions via Jensen's Inequality.
28 Violations of mean-field assumptions mean that parameter estimates from models fit to upscaled
29 data (e.g., eddy covariance towers) are likely systematically biased. Likewise, predictions of CO₂
30 efflux from models conditioned on mean-field values will also be biased. Here we present a
31 generic mathematical analysis of upscaling Michaelis-Menten kinetics under heterogeneity and
32 provide solutions in dimensionless form. We illustrate how our dimensionless form facilitates
33 qualitative insight into the significance of this scale transition and argue that it will facilitate
34 cross site intercomparisons of flux data. We also identify the critical terms that need to be
35 constrained in order to unbiased parameter estimates.

36 **1 Introduction**

37 The current crisis of anthropogenic climate change is expected to accelerate during the 21st
38 century. Despite considerable effort to better constrain global biogeochemical models,
39 considerable uncertainty remains about how best to represent emerging mechanistic
40 understanding of soil element cycling into process-based models (Wieder et al., 2015; Todd-
41 Brown et al., 2018). This is a critical gap in knowledge because variations among models predict
42 hugely varying responses to global change drivers such as temperature, soil moisture, and CO₂
43 enrichment. For example, a traditional first-order linear model forecasts no change or even slight
44 enhancement of soil organic carbon (SOC) pools by 2100 whereas one microbial-explicit model
45 forecasts a loss of ~70Pg of carbon (C), depending on whether microbial physiology acclimates
46 to higher temperatures (Wieder et al., 2013). In general, our understanding of how carbon (and
47 other elements) cycles in soil is undergoing significant revision toward a more microbial-centric
48 paradigm. In contrast to traditional first-order linear models (e.g. CENTURY, Parton et al.,
49 1987), microbial explicit models feature non-linear dynamics in which microbial biomass (or,
50 similarly, microbially-driven enzyme pools) are responsible for decomposition, in addition to
51 providing substrate for synthesis of potentially long-term SOC (Blankinship and Schimel, 2018;
52 Blankinship et al., 2018). While indisputably a better representation of our scientific knowledge,
53 non-linear microbial models face several well-known challenges, including less analytical
54 tractability, greater computational challenges, and uncertainty about structural formulation and
55 dynamics (Georgiou et al., 2017; Sihi et al., 2016; Wang et al., 2014). However, one critical
56 consequence of non-linear microbial models that is only recently gaining attention is their
57 implications for addressing the upscaling challenge.

58 While the fields of population and community ecology have long confronted the challenges
59 posed by non-linearity and heterogeneity in spatiotemporal scaling of ecological dynamics
60 (Chesson, 2009; Levin, 1992), ecosystem ecology and biogeochemistry have tended to approach
61 the challenge of scale either by 1) utilizing mean-field assumptions, or 2) addressing the

62 challenge of scaling via grid-based computational/numeric methods. While there is nothing
63 wrong inherently with either approach, they unfortunately cannot yield theoretical insight into
64 the consequences of non-linearity and heterogeneity for scaling. Briefly, the combination of non-
65 linearity and heterogeneity means that aggregated behavior differs systematically from mean-
66 field predictions, a special case of Jensen’s Inequality. In mathematical notation:

$$67 \quad E[f(x)] \neq f(E[x]) \quad (1)$$

68 Although Jensen’s Inequality is well-known from basic probability theory (Ross, 2002) it’s
69 implications for ecological dynamics under heterogeneity were not well-appreciated until the
70 pioneering work of Peter Chesson in the 1990s (Chesson, 1998). In the case of carbon cycle
71 science, there are a few immediate and critical applications. For instance, most trace gas
72 emission processes are well-known to be non-linear functions of underlying drivers such as
73 temperature and soil moisture. For example, ecosystem respiration is an exponential function of
74 temperature (usually expressed in Q_{10}), and a unimodal function of soil moisture. Thus, when
75 matching observations of CO_2 efflux (“ F ”) to ecosystems, variations in soil temperature and
76 moisture could imply that F differs systematically from a mean-field prediction. Likewise,
77 variations in biotic interactions between microbes likely play a key role in biogeochemical
78 cycling (Buchkowski et al. 2017). In addition to missing critical analytical insight, not
79 accounting for this behavior might have severe consequences for inverse modeling and
80 estimation of the parameters governing process-based models (Bradford et al., 2021). Moreover,
81 a significant advance in recent research has focused not only on microbial-explicit formulations,
82 but the role of microbe-substrate collocation in the complex and heterogeneous soil environment
83 in both the synthesis and decomposition of organic matter (Schimel and Schaeffer 2012,
84 Lehmann et al. 2020). This spatial collocation itself has very important implications for scale
85 transitions in soil systems, and thus requires specific theoretical attention from this perspective.
86 Overall, the basic consequences of Jensen’s Inequality for estimation of trace gas emission (CH_4
87 and N_2O) were first discussed by Van Oijen et al. (2017), but have not been picked up on
88 elsewhere, until the present work and by Chakrawal et al. (2020)

89 Chakrawal et al. (2020) provide a detailed and compelling first-pass application of scale
90 transition theory to biogeochemical modeling. Our contribution here complements their laudable
91 effort by providing a more generic mathematical analysis of the scale transition, equally
92 applicable to both forward and reverse Michaelis-Menten microbial kinetics. As in Chakrawal et
93 al. (2020), we address the consequences of heterogeneity in both substrate/microbes
94 (“biochemical heterogeneity”) as well as in the kinetic parameters (“ecological heterogeneity”).
95 However, we diverge from their approach in that, rather than explore detailed simulation models,
96 we derive a completely non-dimensionalized expression for aggregating non-linear microbial
97 kinetics over both types of heterogeneity simultaneously. We illustrate the clarity this brings in
98 several special cases of our full analysis. Altogether, our approach provides new insight into the
99 properties of the scale transition and enables clear conclusions to be drawn across systems in
100 terms of the role of spatial variances and covariances in shaping ecosystem carbon efflux. Our
101 work provides a simplified, yet systematic framework around which to base subsequent
102 empirical and simulation-based studies.

103 **2. Carbon Efflux and the Scale Transition**

104 A variety of microbial-explicit process-based models have been proposed in the literature,
 105 starting with the classic enzyme pool model of Schimel and Weintraub (2003). In order to
 106 elucidate universal properties of the scale transition, we focus here on the CO_2 efflux following
 107 decomposition of a single substrate by a single microbial pool obeying Michaelis-Menten (MM)
 108 dynamics:

109
$$F = -f(C, MB, \theta) \tag{2}$$

110

111 where F is the CO_2 flux, C is the carbon substrate, MB the live microbial biomass, θ is a vector
 112 of parameters, specifically V_{max} (the maximum reaction rate given saturation of either C , in
 113 forward MM, or microbial biomass (MB), in reverse MM), k_h (the half-saturation constant), and
 114 carbon-use efficiency, ϵ .

115 Our specific model for F is:

116
$$F = (1 - \epsilon) \times C \times \frac{V_{max}MB}{k_h + MB} \tag{3}$$

117

118 Following the terminology of Chesson (1998,2012), the above is our “patch” model and our goal
 119 is to understand how spatial variances and covariances impact the integrated flux, which
 120 represents the spatial expectation or $E[F]$ (hereafter denoted \bar{F}), which represents

121
$$\bar{F} = \overline{-C \times (1 - \epsilon) \times \frac{V_{max}MB}{k_h + MB}} \tag{4}$$

122 Where the bar over the expression represents the mean. The incorrect approach to solving for
 123 $E[F]$ is to simply plug-in the mean-field solution:

124
$$\bar{F} = \overline{-C} \times \overline{(1 - \epsilon)} \times \frac{\overline{V_{max}} \overline{MB}}{\overline{k_h} + \overline{MB}} \tag{5}$$

125

126 Analytically, an exact solution would require specification of a joint distribution for C , MB and
 127 parameters, $\pi(MB, C, \theta)$, and solution of the convolution integral:

128
$$\iiint -f(MB, C, \theta)\pi(MB, C, \theta)dMBdCd\theta \tag{6}$$

129

130 However, following Chesson (2012) and Chakrawal et al. (2019) we are free to approximate the
 131 solution for arbitrary distributions using a Taylor Series approximation expanded to the 2nd
 132 moment. Specifically, we take the expectation over a multivariable Taylor Series expansion,

133 centered around the mean-field values of all parameters θ (for simplicity, the variables MB and
 134 C are included in the parameter vector θ):

$$135 \quad \bar{F} \approx E \left[f(\bar{\theta}) + \frac{1}{2} \theta_{\theta-\bar{\theta}}^T H_{\bar{\theta}} [f(\theta)] \theta_{\theta-\bar{\theta}} \right] \quad (7)$$

136

137 where $H[f(\theta)]$ represents the Hessian matrix of the function that determines the CO_2 efflux F
 138 (in this case Michaelis-Menten), $\theta_{\theta-\bar{\theta}}$ represents the deviation from the mean at each instance
 139 and for each of the parameters. It can easily be seen that $\theta_{\theta-\bar{\theta}}^T \times \theta_{\theta-\bar{\theta}}$ is the variance-covariance
 140 matrix, and that the first moment of the Taylor expansion cancels because the first derivative of
 141 $\theta_{\theta-\bar{\theta}}$ is zero.

142 2.1 Non-dimensionalization

143 Expanding equation 7 out, we have 5 terms involving the variances of C , MB , $1 - \varepsilon$, V_{max} , and
 144 k_h , and 10 terms involving covariances among the parameters. We can redistribute the
 145 expectation operator over this approximation to see that we are dealing with the contributions
 146 from the variance-covariance terms, weighted by the second partial derivatives evaluated at the
 147 mean for each parameter. However, the resulting expression **does not readily yield insight into**
 148 **the impact of scale transition upon the dynamics**, since second partial derivatives and cross
 149 partial derivatives do not have easy intuition. Moreover, variances and covariances depend
 150 arbitrarily upon the scale of units and measurements involved, hindering both intuition and cross-
 151 site comparisons. Therefore, we non-dimensionalize equation 7 for \bar{F} as follows:

- 152 1) We define a dimensionless quantity λ as $\frac{MB}{k_h}$. λ thus represents a multiplicative factor
 153 expressing the ratio of the mean microbial biomass over its half-saturation value, indicating
 154 the microbial saturation for the decomposition.
- 155 2) We divide all of the terms in 6 by their mean-field value, and represent the whole equation
 156 as a product:

$$157 \quad \bar{F} \approx f(\bar{\theta}) + f(\bar{\theta}) \left((\theta - \bar{\theta})^T \frac{\partial^2 f}{\partial \theta^2 \theta = \bar{\theta}} (\theta - \bar{\theta}) \right) = f(\bar{\theta}) \left(1 + \left((\theta - \bar{\theta})^T \frac{\partial^2 f}{\partial \theta^2 \theta = \bar{\theta}} (\theta - \bar{\theta}) \right) \right)$$

158 (8)

- 159 3) We calculate the resulting expression for \bar{F}
- 160 4) We notice that $\frac{Var(\theta)}{\bar{\theta}^2}$ can be re-expressed as $\left(\frac{SD(\theta)}{\bar{\theta}} \right)^2$ which in turn is the square of the
 161 dimensionless coefficient of variation $(CV(\theta))^2$. This enables us to reformulate the
 162 variance terms in (7).
- 163 5) Similarly, since the covariance terms can be rewritten as $COV(X, Y) = \rho_{X,Y} SD(X) SD(Y)$,
 164 we have the following equality:

$$165 \quad \frac{COV(X, Y)}{\bar{X}\bar{Y}} = \rho_{X,Y} CV(X) CV(Y) \quad (9)$$

166

167 Applying steps 1-5 to all the terms in the equation, we end up with a fully dimensionless
168 equation:

$$\begin{aligned} 169 \quad \bar{F} \approx f(\bar{\theta}) & \left(1 + \frac{\lambda}{(1+\lambda)^2} [\rho_{k_h, MB} CV(k_h) CV(MB) - CV(MB)^2] + \frac{1}{(1+\lambda)^2} [CV(k_h)^2 - \right. \\ 170 \quad & \left. \rho_{k_h, MB} CV(h) CV(MB)] + \frac{1}{(1+\lambda)} [\rho_{C, MB} CV(C) CV(MB) + \rho_{V_m, MB} CV(V_m) CV(MB) + \right. \\ 171 \quad & \left. \rho_{\epsilon, MB} CV(\epsilon) CV(MB) + \rho_{C, k_h} CV(C) CV(k_h) - \rho_{V_m, k_h} CV(V_m) CV(k_h) - \rho_{k_h, \epsilon} CV(k_h) CV(\epsilon)] + \right. \\ 172 \quad & \left. \rho_{V_m, C} CV(V_m) CV(C) + \rho_{C, \epsilon} CV(C) CV(\epsilon) + \rho_{\epsilon, V_m} CV(\epsilon) CV(V_m) \right) \end{aligned} \quad (10)$$

174

175 Note that by symmetry, we have also solved for the case of the forward Michaelis-Menten
176 kinetics. This can be expressed simply by interchanging C and MB , and by correspondingly
177 altering λ to represent the ratio of substrate availability over half-saturation.

178 3. Discussion

179 Having fully non-dimensionalized equation 7, we are in a much better position to gain analytical
180 insight into the scale transition. To begin, we note the pivotal role played by the quantity λ
181 throughout this equation. λ scales the contributions of the parameter variation and correlation
182 terms to the deviation from mean field behavior according to the ratios $\frac{\lambda}{(1+\lambda)^2}$, $\frac{1}{(1+\lambda)^2}$, and $\frac{1}{1+\lambda}$. All
183 of the parameter variance terms (which have become $CV(\theta)^2$ upon non-dimensionalization), are
184 scaled by one of these three λ ratios, alongside 7 out of 10 of the covariance terms. Overall, low
185 λ (here $\lambda < \approx 1$) keeps all the spatial correction terms in play, while increasing λ tends to
186 simplify matters. As noted by others (Sihi et al., 2016; Buchkowski et al., 2017), as $MB \rightarrow \infty$
187 (equivalent to $MB \gg k_h$ or $\lambda \rightarrow \infty$), reverse Michaelis-Menten kinetics converge to first order,
188 leaving:

$$189 \quad \bar{F} = -C \times (1 - \epsilon) \times V_{max} \quad (11)$$

190 Accordingly, in our setup, the multiplicative factor for the scale transition correction approaches
191 a simplified expression, as $\lambda \rightarrow \infty$:

$$192 \quad \bar{F} \rightarrow f(\bar{\theta}) \left(1 + \rho_{V_m, C} CV(V_m) CV(C) + \rho_{C, \epsilon} CV(C) CV(\epsilon) + \rho_{\epsilon, V_m} CV(\epsilon) CV(V_m) \right) \quad (12)$$

193 This is quite remarkable. Despite invoking the situation where microbial biomass (and its
194 enzyme supply) is effectively infinite - thus linearizing the underlying patch models - we cannot
195 eliminate the possibility of a potentially substantial deviation from mean-field when scaling
196 decomposition kinetics. We note that in this resulting expression, we have reduced the situation
197 to a set of three critical correlations involving two microbial physiological parameters (ϵ , and
198 V_m), and substrate availability (C). Regardless of their respective variabilities (CV terms), if
199 these correlations are close to zero, then the whole expression converges to mean field.

200 Returning to the situation where λ is not large, if we ignore the correlation terms (temporarily
 201 setting to zero), we see that there are direct contributions to the scale transition from the
 202 variability in MB and k_h that may, to some extent, balance each other:

$$203 \quad \bar{F} = f(\bar{\theta}) \left(1 + \frac{1}{(1+\lambda)^2} [CV(k_h)^2] - \frac{\lambda}{(1+\lambda)^2} [CV(MB)^2] \right) \quad (13)$$

204 Focusing on the offsetting correction terms, we can re-write as:

$$205 \quad \frac{\lambda}{(1+\lambda)^2} \left[\frac{CV(k_h)^2}{\lambda} - CV(MB)^2 \right] \quad (14)$$

206 and for the case of $\lambda = 1$, this becomes:

$$207 \quad \frac{1}{4} [CV(k_h)^2 - CV(MB)^2] \quad (15)$$

208 Thus, variability in the factors of soil protection that impact upon k_h in practice, can offset the
 209 impact of variability in microbial biomass itself.

210 More generally, starting with our dimensionless equation 10 puts modelers and empiricists in a
 211 better position to assess the quantitative significance of the scale transition correction across
 212 systems compared to expressions with opaque second partial derivatives and cross derivatives,
 213 and arbitrarily scaled variance terms. By re-expressing \bar{F} in terms of dimensionless coefficients
 214 of variation, correlation coefficients and λ , we can plug-in realistic values for variability in any
 215 relevant parameter and assess the % effect on \bar{F} in terms of deviation from mean field behavior.
 216 We argue that this formulation possesses significant advantages not only in understanding how
 217 to scale flux estimates (\bar{F}) *within* a site, but going forward will help facilitate intercomparison
 218 *among* sites in terms of their scale-free variability. In particular, we explore variation in
 219 dominant environmental drivers of inter-site variation (temperature and soil moisture) below. But
 220 first, we analyze how the scale transition sheds new light on microbe-substrate collocation.

221 3.1 Spatial Collocation of Microbes and Substrate

222 To illustrate these advantages in interpretability, we first take the special case of a model where
 223 we treat all parameters as constant (and known) except substrate and microbial biomass. This
 224 corresponds to setting the other CV and ρ terms to 0. In this case, we are isolating the impact of
 225 the spatial collocation of substrate and decomposers. Our equation becomes:

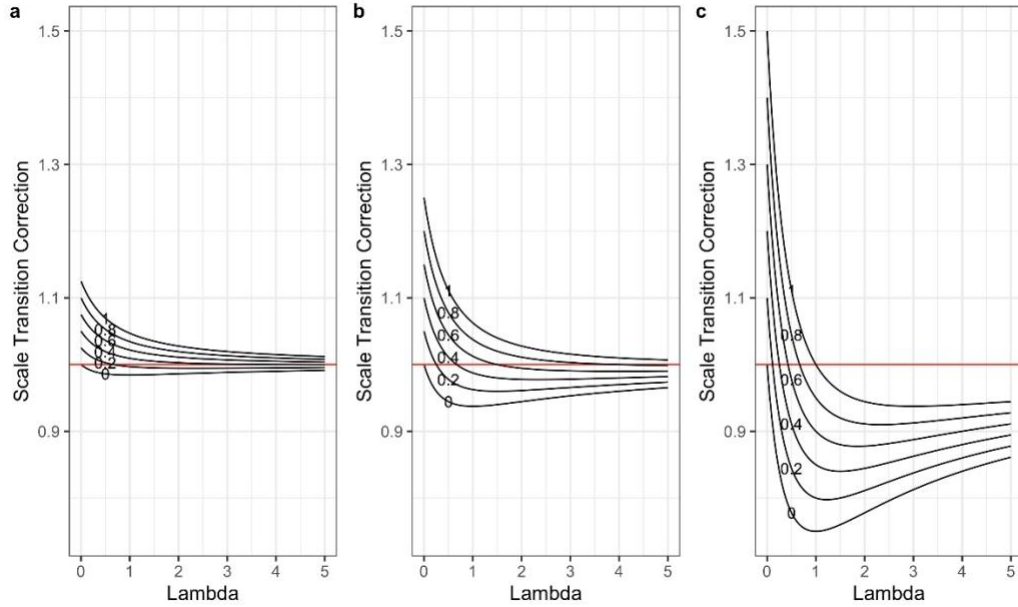
$$226 \quad \bar{F} \approx f(\bar{\theta}) \left(1 - \frac{\lambda}{(1+\lambda)^2} CV(MB)^2 + \frac{1}{(1+\lambda)} (\rho_{C,MB} CV(C) CV(MB)) \right) \quad (16)$$

227 In the case of this formulation, there is a very clear dual convergence as λ increases:

- 228 1. deviation from mean-field behavior declines, and
- 229 2. first order kinetics are approached

230 Indeed, our equation 16 reveals the exact speed of this convergence in terms of dimensionless λ
 231 and a balance of $CV(MB)$, $CV(C)$ and their correlation.

232 We illustrate the scale transition solutions to equation 16 as a function of λ for various choices of
 233 $CV(C)$, $CV(MB)$ and ρ in Fig. 1:



234

235 *Figure 1: Scale transition correction for models given spatial collocation between microbes and*
 236 *substrate across a gradient of λ values, and for a variety of correlation ρ values (0-1), with*
 237 *$CV(SOC)$ held constant at 0.5, a) $CV(MB) = 0.25$, b) $CV(MB) = 0.5$, and c) $CV(MB) = 1$. Note*
 238 *that in panel c) the system appears to converge on a value lower than 1. However, as λ*
 239 *increases, convergence to 1 does occur, albeit slowly, as it must according to equation 16.*

240 In the case of pure spatial collocation, with no variation in the kinetic parameters, the scale
 241 transition correction factor varies from a maximum of 1.5 to a minimum around 0.75, and in all
 242 cases indeed converges to 1 as λ increases. The variability assumed for C and MB impacts only
 243 the scale of the correction factor, not the qualitative behavior as λ and ρ vary. One benefit of
 244 having a simplified, generic dimensionless equation of this sort is that it enables us to think in a
 245 unit-free/scale-free manner about the *plausible* range of the scale transition correction given
 246 transparent assumptions about variability and correlations.

247 Another benefit is that it is mathematically tractable to see how the variance and covariance
 248 terms can balance each other, and to solve for where they are equal. If we introduce a new term
 249 λ_2 representing the relationship between $CV(MB)$ and $CV(C)$ as follows $CV(MB) = \lambda_2 CV(C)$,
 250 we can re-express the the deviation of the mean-field correction from 1 as:

251
$$CV(MB)^2 \left[\frac{1}{1+\lambda} \left(\rho \lambda_2 - \frac{\lambda}{(1+\lambda)} \right) \right] \quad (17)$$

252 Thus, whether the correction is positive or negative depends crucially on the product of the
 253 collocation correlation coefficient ρ and the extent of variability in substrate relative to variability
 254 in microbes.

255 If we fix λ to unity, as done in our Fig.1, our mean-field deviation simplifies to:

256
$$CV(MB)^2 \left[\frac{1}{2} \left(\rho \lambda_2 - \frac{1}{2} \right) \right] \quad (18)$$

257 In general, the scale transition correction is larger to the extent that microbial variability exceeds
 258 substrate variability under reverse Michaelis-Menten kinetics (the opposite relation holds for
 259 forward Michaelis-Menten by symmetry). Thus, variability in microbial biomass is not only
 260 important by itself in driving Jensen's Inequality, but also with respect to variability in substrate
 261 supply. **Our analysis thus highlights another route of convergence back to the mean field**
 262 **beyond the simple increase of λ : variability in substrate increasing to match variability in**
 263 **microbes in the presence of positive spatial colocation factor.** We also note that the
 264 magnitude of the scale transition correction scales as the *square* of the coefficient of variation of
 265 microbial biomass. Quadratic scaling means that at low to moderate levels of variability, the
 266 deviation from mean field behavior is likely to be minimal, but at moderately high to high levels
 267 of variability, severe deviations can be expected. Finally, we note that throughout, our
 268 development of these kinetics assume proportionality to microbial biomass, but it is really the
 269 live/active fraction that matters. Since the active fraction vary considerably with environmental
 270 conditions (e.g. soil temperature and moisture explored below), we believe it is reasonable to
 271 expect large coefficients of variation overall in most real-world ecosystems.

272 **3.2 Environmental Heterogeneity**

273 So far, we have analyzed in depth the role of variability in microbes and their substrate, but not
 274 in the ecological drivers underlying maximal reaction rates (i.e. V_{max}) or half-saturation (i.e. k_h).
 275 We start with the observation that both linear first order and non-linear microbial models will
 276 show characteristic scale transitions given heterogeneity in temperature and soil moisture.
 277 Consider the asymptotic convergence of the reverse MM to first order

$$278 \quad \frac{dC}{dt} = -V_{max}\bar{C} \quad (19)$$

279 This is mathematically equivalent to the more standard way of writing these models down as

$$280 \quad \frac{dC}{dt} = -kC \quad (20)$$

281 In the analysis that follows, we will consider both temperature and soil moisture as factors that
 282 could drive variations in V_{max} over space or time.

283

284 **3.2.1 Scale Transition over Temperature Heterogeneity**

285 To make matters clear, we re-express the rate limiting maximal reaction velocity V_{max} first as a
 286 function of temperature (assuming all else constant):

$$287 \quad V_{max} = e^{aT} \quad (21)$$

288 In this case, our integrated flux equation will be:

$$289 \quad \frac{\overline{dC}}{dt} = -e^{aT} \times (1 - \epsilon) \times C \quad (22)$$

290 Allowing for variability in T , this integrated equation will show characteristic scale transitions
 291 given the convex (exponential) relationship with T .

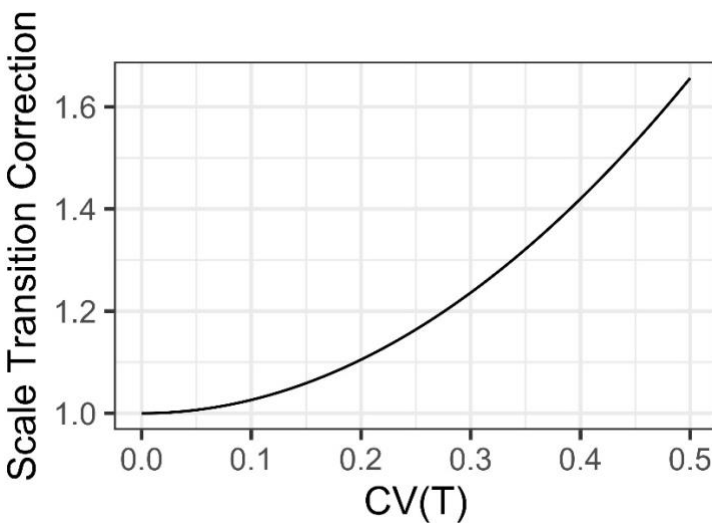
292 Using the Taylor expansion again to second order we have:

$$293 \quad \overline{V_{max}} \approx e^{a\bar{T}} \left(1 + \frac{1}{2} a^2 \text{Var}(T)\right) \quad (23)$$

294 The critical scale transition correction term here is again multiplicative, and we re-express it into
295 a function of a dimensionless coefficient of variation parameter more suited to ready
296 interpretation. First, the exponential dependence of respiration on temperature is canonically
297 codified in terms of Q_{10} scaling. We substitute $a = \frac{\log(Q_{10})}{10}$, and end up with:

$$298 \quad 1 + \frac{1}{2} a^2 \text{Var}(T) = 1 + \frac{1}{2} \left(\frac{\log(Q_{10})}{10}\right)^2 \text{Var}(T) = 1 + \frac{1}{200} (\log(Q_{10}))^2 (SD(T))^2 =$$
$$299 \quad 1 + \frac{1}{200} (\log(Q_{10}))^2 (\bar{T} CV(T))^2 \quad (24)$$

300 For a “typical” Q_{10} of 2.5, and a \bar{T} of 25, we see the multiplicative scale transition correction in
301 figure 2:



302

303 *Figure 2: Scale transition correction for Q_{10} temperature response scaling given coefficient of*
304 *variation $CV(\text{Temp})$ from 0 to 0.5*

305 As is clear in Fig. 2, the scale transition for temperature is extremely convex. Integration of
306 fluxes over ecosystems with significant heterogeneity in temperature invokes substantial
307 deviation from a mean-field model. For instance, at a CV of 0.2, the scale transition correction is
308 1.10, but by a CV of 0.5 it is 1.66. Obviously, the significance of this depends on the scale and
309 heterogeneity over which an accurate flux model is desired. For a smaller footprint eddy
310 covariance tower (e.g. Gomez-Casanovas et al., 2018) over a uniform habitat type, soil (and near
311 surface) temperatures probably do not vary by much more than 20%. Regardless, our general
312 mathematical analysis quantifies and clarifies exactly how the scale of variation influences the
313 degree of the scale transition correction.

314 Notably, the only difference between the scale transition correction for first order and for reverse
315 Michaelis-Menten kinetics is that in the latter there would be additional correlation terms to

316 consider, e.g. the correlation between temperature and V_{max} , temperature and k_h , as well as
317 temperature and C and MB .

318 3.2.2 Scale Transition over Soil Moisture Heterogeneity

319 Unlike soil temperature, we expect heterotrophic respiration to respond in a unimodal fashion to
320 soil moisture. At low levels of soil moisture, microbes are moisture limited, and at high levels
321 they are oxygen limited, with some optimum range of values in the middle. Although a
322 considerable amount of work has gone into developing soil moisture functions, including both
323 empirical and theoretical derivations (Yan et al., 2018; Tang and Riley, 2019), there is no clear
324 consensus on an optimal representation. Moreover, many of the candidate functions complicate
325 analysis considerably by virtue of stepwise formulation (Linn and Doran, 1984). Therefore, to
326 study the implications of the scale transition we proceed via a powerful simplifying abstraction,
327 and simply represent the soil moisture response as a quadratic of the form:

$$328 \quad V_{max} = \beta\phi - \beta\phi^2 \quad (25)$$

329 where ϕ represents the soil moisture content. We normalize our function in two senses: first in
330 output space we assume that it has a maximum of 1 (i.e. represents heterotrophic respiration
331 relative to a maximum value of 1), and second that the soil moisture content ϕ is itself bounded
332 between 0 and 1, with a peak in the middle at 0.5. Thus, our function captures the unimodal
333 abstraction in a symmetric form. Given these conditions, there is a unique solution at $\beta = 4$.

334 We seek the scale transition:

$$335 \quad \overline{V_{max}} = \overline{4\phi - 4\phi^2} \quad (26)$$

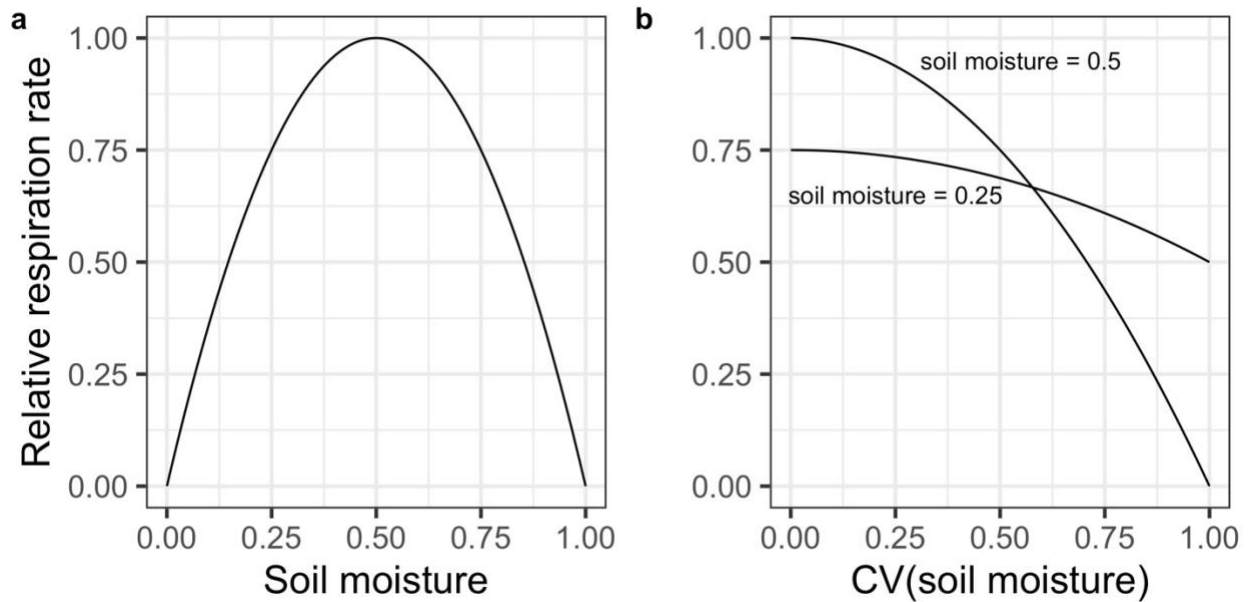
336 As before, we can approximate this as a mean-field plus a correction to the mean field, which
337 after some re-writing becomes:

$$338 \quad \overline{V_{max}} \cong 4(\overline{\phi} - \overline{\phi}^2 - Var(\phi)) \quad (27)$$

339 We then substitute: $Var(\phi) = \overline{\phi}^2 CV(\phi)^2$, and re-express:

$$340 \quad \overline{V_{max}} \cong 4(\overline{\phi} - \overline{\phi}^2(1 + CV(\phi)^2)) \quad (28)$$

341



342 *Figure 3: a. heterotrophic respiration as a function of soil moisture given solution in equation*
 343 *25. Note that soil moisture is normalized with a maximum response at 0.5, where 1 represents*
 344 *complete waterlogging, and respiration is normalized to a maximum of 1. b. Scale transition*
 345 *approximate solution for respiration as a function of the dimensionless coefficient of variation of*
 346 *soil moisture where mean field soil moisture is either 0.5 (top curve) or 0.25 (bottom curve,*
 347 *equivalent to 0.75 by symmetry).*

348 As shown in Fig. 3, where mean field soil moisture is close to the optimal value, scale transition
 349 effects are expected to be quite large. For instance, by the time the coefficient of variation is 0.5,
 350 efflux would only be 75%, and declines rapidly to 0 as the coefficient of variation approaches 1.
 351 Clearly, this latter outcome is not necessarily biologically realistic, and a more detailed
 352 numerical experiment should be done to explore scenarios with that much variation. However,
 353 our abstractions yield the simple insight that mean-field solutions invariably *overestimate* the
 354 real flux, and this overestimation can be considerable. In our experience, soil moisture varies
 355 tremendously both over space, especially given contrasts in topography, relief and underlying
 356 soils, but perhaps even more so over time, including within a small area, due to day-day and even
 357 hour-by-hour variations in precipitation, evapotranspiration and drainage. To the extent that
 358 ecosystems deviate from a stable, consistent soil moisture regime, we should expect strong scale
 359 transition effects.

360 Our results on soil moisture relate to the argument by Tang and Riley (2019) that heterotrophic
 361 respiration arises from a two-step process whereby substrate must diffuse into the vicinity of
 362 microbes, and then be taken up – the latter by a Michaelis-Menten kinetic. However, microscale
 363 variations in soil moisture mediate and regulate the first step of the process, so that the “effective
 364 substrate affinity” (the k_h term in the Michaelis-Menten model) deviates from the base substrate
 365 affinity of the second step. Tang and Riley (2019) point out that the effective substrate affinity
 366 therefore reflects microscale heterogeneity, and they argue that experimentalists should account
 367 for this when fitting efflux data to models. But what about scaling up in the field from small
 368 plots to fields to larger ecosystem units? Fortunately, our analytical framework can be readily
 369 queried to account for heterogeneity in substrate affinity (k_h).

370 3.2.2.1 Heterogeneity in Substrate Affinity

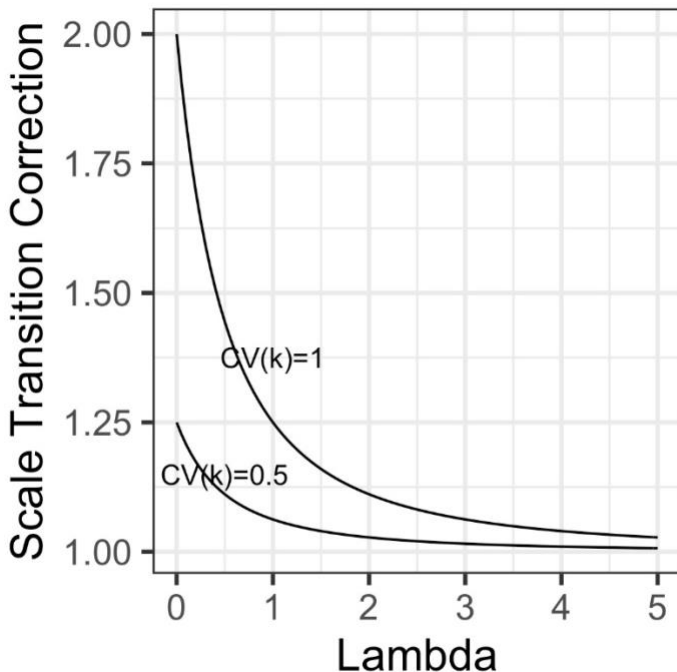
371 We proceed by first by holding all terms constant except allowing the half saturation constant k_h
372 to vary, reflecting variations in soil moisture, or frankly any other factor regulating microbial
373 access to substrate (e.g. soil aggregation, organomineral complexes, etc. Schmidt et al., 2011,
374 Lehmann et al., 2020). As usual, we seek the scale transition over $\frac{V_{max}MB}{k_h+MB} = f(k_h)$. We can
375 recover this transition quickly from equation (10) by extracting only the term with (k_h) , or
376 rederive from scratch holding everything else as constant. The result is that the dimensionless
377 scale transition correction term is:

$$378 \quad 1 + \frac{1}{(1+\lambda)^2} CV(k_h)^2 \quad (29)$$

379 Intriguingly, this result shows that heterogeneity in substrate affinity *per se* results in a convex
380 correction term, implying that mean-field models will under-estimate rather than overestimate
381 the resulting fluxes. Given that the correction is proportional to the inverse of the square of λ ,
382 this correction converges rapidly to 1 (no scale transition) as mean microbial biomass increases
383 (Figure 4). Nevertheless, where heterogeneity is high and λ is around 1 or lower, the correction
384 could be substantial.

385 More broadly, our analysis highlights that, under non-linear Michaelis-Menten kinetics for
386 representing carbon processing, the impact of environmental heterogeneity acting on the
387 substrate affinity parameter is opposite of when it acts on the V_{max} parameter. Thus, if we
388 represent soil moisture as a modifier to the V_{max} in the numerator, heterogeneity in soil moisture
389 should result in lower carbon efflux than mean field, whereas if we represent soil moisture
390 heterogeneity by way of substrate affinity it is the opposite. At first glance, this finding appears
391 inconsistent with Tang and Riley (2019). However, we note that their full kinetic formulations
392 include soil moisture acting in both roles ultimately, and therefore resulting in the familiar
393 unimodal soil moisture-respiration relationship. For instance, their application of ‘Dual Monod’
394 kinetics include soil moisture driving effective substrate affinity terms for both carbon and water,
395 as well as an effective fraction of active microbes (which modifies the numerator).

396 Thus, for the analysis of upscaling fluxes in the presence of soil moisture heterogeneity, we
397 expect the concave corrections of Figure 3b to hold, regardless of the fine-scale details of the soil
398 moisture function used.



399

400 *Figure 4: Scale transition factor for variations in the substrate affinity (“k”) parameter in*
 401 *Michaelis-Menten kinetics as a function of dimensionless λ (the ratio of mean-field microbial*
 402 *biomass over mean-field k), for two scenarios of variability in affinity, one where coefficient of*
 403 *variation = 1 (top curve), the other where coefficient of variation = 0.5 (bottom curve).*

404 3.3 Lessons for Scientific Inference

405 We close our discussion by considering the implications of the scale transition for advancing the
 406 state of biogeochemical modeling. Critically, the representation of non-linear (microbial driven)
 407 kinetics is a crucial modeling choice with large implications for long-term SOC forecasts.
 408 Traditional first-order process-based models dodge explicit representation of these kinetics, but
 409 nonetheless have worked well in practice. This state of affairs persists because both non-linear
 410 and linear kinetics are capable of representing coarse-scaled biogeochemistry reasonably well, at
 411 least in certain respects. Since first order kinetics are known to be a crude approximation, the
 412 crucial question for practice is not whether they are “true”, but rather whether there is significant,
 413 systematic information loss inherent to their use. Fortunately, the scale transition offers a clear,
 414 clean path to discriminate between these alternative model formulations.

415 As noted throughout, the dimensionless term λ plays a critical role in linking the non-linear
 416 (Michaelis-Menten) kinetics to the first order kinetics. As λ increases, the non-linear kinetics
 417 converge to first order. Thus, in seeking to infer where the non-linear kinetic models provide
 418 substantial advantages, ensuring that λ is not too large ($\gg 1$) is the first priority.

419 Previous work Sihi et al. (2016) has approached this question theoretically, from first principles.
 420 Here, we point out that demonstrating substantial deviation from mean-field model when fitting

421 non-linear kinetics to data is both a necessary and sufficient condition for inferring that λ is not
422 too large. Thus, we recommend that time series of flux data be fit to both a first order and a non-
423 linear kinetic model, where crucial covariates including substrate (SOC), microbial biomass, and
424 possibly environmental parameters such as temperature, have been measured sufficiently well to
425 quantify the relevant variances and covariances. Where predictive performance and forecasting
426 are the primary goals, we recommend careful consideration of model parameterizations
427 (i.e. based on leave-one-out cross validation), and model combination via “stacking” where it is
428 difficult to infer a decisive “winner” (Yao et al., 2018) acknowledging that carrying this out is a
429 significant enterprise.

430 In addition to the role of λ , our analysis also cleanly shows the contribution of other terms to the
431 scale transition, and thus alternative metrics to assess. First and foremost, accounting for the
432 spatial collocation of microbial biomass and substrate (according to equation 16 above) or the
433 various correlation terms between microbial biomass and kinetic/environmental factors in
434 equation 10. Moreover, recent theoretical developments offer quantitative insights into the
435 interpretation of the half saturation constant (or the substrate affinity parameter) and thus
436 λ (Tang and Riley, 2019). Tang and Riley (2019) decompose microbial access to substrate into a
437 two-step process, which is often strongly modified by soil moisture. Moreover, conceptual
438 advances suggest that collocation is a potentially important factor in organic matter
439 decomposition vs. stabilization (Schimel and Schaeffer 2012, Lehmann et al. 2020). Here, we
440 show that both affinity and collocation are co-dependent in their effects on scale transition.

441 In addition to fitting fully parameterized flux models (as above), simpler statistical models could
442 be fit examining the role of variations in microbial biomass, or collocation of microbial biomass
443 and SOC, in explaining across-site variations in ecosystem respiratory fluxes (F). **A substantial**
444 **role for either correlation of MB and C, or their variability, would constitute ipso facto**
445 **evidence of the preferability of well-formulated non-linear kinetic models.** On the other
446 hand, small roles for collocation, or evidence of large values of λ in practice would suggest
447 minimal advantage to abandoning first order models in favor of more complex microbial models.
448 A meta-analytical approach across sites will benefit greatly from our formulation in terms of
449 dimensionless quantities like λ and the various coefficients of variation.

450 We further note that the scale transition presented here is closely related to global sensitivity
451 analysis (GSA, Saltelli et al. 2010). In its fundamental setup, a GSA tests effects of variability in
452 parameters. While GSA has been typically used towards characterizing the uncertainty of
453 parameters, it is directly applicable to spatial and temporal variability. For example, the first
454 order results of a GSA (or the result of a one at a time parameter substitution), provides the
455 contribution of that parameter to the scale transition. Similarly, the ‘all but one’ perturbation
456 offers insights into how the net effect of all parameters (and variables) violates the mean field
457 approximation. Therefore, a computationally expensive GSA can be leveraged to garner further
458 insights on top of sensitivity effects, allowing for the characterization of the scale transition.
459 Indeed, a computationally intensive approach to simulating scale transitions was utilized by
460 Chakrawal et al. (2020) to good effect. However, we suggest future computational studies build
461 off of the dimensionless approach studied here, including those extended to multiple microbial
462 populations which would result in multiple dimensionless lambdas and corresponding
463 multiplicative contributions to the scale transition. Obviously, the parameter space needs to be
464 properly chosen (or subsetted) to reflect appropriate means, variabilities, and perhaps most

465 challenging - correlations. Equation 10 would then provide analytical, albeit approximate, insight
466 into the scale transition effects, while the GSA would enable study of any shortcomings from
467 approximation, and also allow for quantification of individual variable importance for those
468 parameters that enter into the dynamics in multiple places.

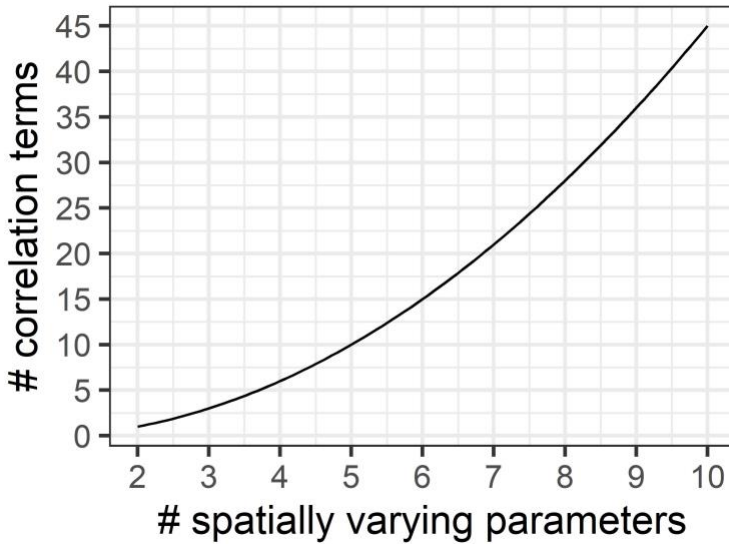
469 Finally, our analysis of environmental factors including temperature and soil moisture leads to
470 readily testable predictions. For temperature, the scale transition is convex and thus, *ceteris*
471 *paribus*, variation in soil temperature should lead to greater effluxes than mean field models
472 would predict. The implications of this for climate-feedback should be studied in greater detail.
473 For soil moisture, which varies considerably across both space and especially time, our analysis
474 based on an idealized quadratic representation yields a concave scale transition correction, i.e.
475 the mean-field soil moisture will over-estimate efflux. Likewise, when represented in both
476 substrate affinity and multiplicative active microbial biomass fraction terms, as in Tang and
477 Riley (2019), the scale transition remains concave. However, environmental factors that act only
478 through substrate affinity would result in a convex correction as in Figure 4. Once again, we
479 highlight that the nature of scaling corrections, wherever it is possible to be studied empirically,
480 can provide insight into the most productive representations of our models.

481 **4. Conclusions**

482 Here, we have illustrated how the spatial scale transition can be expressed in dimensionless form,
483 yielding insight into the systematic operation of Jensen's Inequality in upscaling microbial
484 decomposition kinetics. Our analysis has identified the central role of the dimensionless quantity
485 λ - representing the ratio of mean-field microbial biomass over its half-saturation value - in
486 governing the extent of the scale transition correction, expressed here in multiplicative form best
487 facilitating comparison among systems. For somewhat simplified scenarios - such as restricting
488 to spatial collocation of substrate and microbes - as $\lambda \rightarrow \infty$, the mean-field correction goes to 0
489 and the model converges to first order.

490 This dual sense of convergence also provides opportunity to empirically test for the presence of
491 significant non-linear microbial dynamics in upscaled field data: to the extent that upscaled
492 fluxes deviate from the flux estimated at mean-field conditions, we have *ipso facto* evidence for
493 the importance of formulating our biogeochemical models with these non-linear terms.
494 Conversely, where there is close agreement between mean-field and upscaled fluxes, there are
495 arguably stronger reasons for retaining first-order process model formulations.

496 In closing, we would like to point out how this mathematical analysis illustrates the challenge of
497 scaling quite nicely. In the context of non-linear models, for each parameter that is allowed to
498 vary in space, there is not only a new variance parameter, but a number of new covariance terms
499 are induced, growing as the factorial of the number of varying parameters $(5)!$ (Fig. 3). Thus, in
500 the case of the 5 parameter function considered here, the full approximation has 5 mean field
501 terms, 5 coefficients of variation, 10 correlation coefficients, and the dimensionless quantity λ .



502

503 *Figure 3: Model complexity grows exponentially with number of spatially varying parameters.*
 504 *We argue to keep models as simple as possible for both analytical and computational*
 505 *tractability.*

506 Even with a maximally generic and simplified expression, fitting such non-linear time series
 507 models to field data still represents quite a challenge, especially while adequately accounting for
 508 and propagating uncertainty. Modelers and theoreticians should appreciate the complexity of the
 509 task at hand. Fortunately, our analysis has identified a potentially robust route to limiting model
 510 complexity: screen systematically for the importance of various correlations in explaining
 511 variations in fluxes. Accordingly, we recommend that research focus first upon spatial collocation
 512 of MB and C, which is readily measured, and then to thoughtfully and carefully expand models
 513 with additional terms as needed.

514 **Author Contributions:** CHW conceived the original concept, developed the mathematical
 515 analysis, and wrote the manuscript. SG developed the concepts, contributed to the mathematical
 516 analysis, and co-authored and edited the manuscript.

517 **Competing Interests:** None declared.

518 **Acknowledgements:** We stand on the shoulders of giants: Peter Chesson’s research program on
 519 Scale Transition was enormously influential. We thank T. Trevor Caughlin for introducing us to
 520 Chesson’s papers many years ago, and to everyone who has humored discussions of Jensen’s
 521 Inequality ever since. Will Wieder and an anonymous reviewer provided constructive reviews
 522 that improved our manuscript, and Kathe Todd-Brown provided valuable discussion as we
 523 worked through revisions.

524 **References**

525

526 Blankinship, J. C. and Schimel, J. P.: Biotic versus Abiotic Controls on Bioavailable Soil
527 Organic Carbon, 2, 10, <https://doi.org/10.3390/soilsystems2010010>, 2018.

528 Blankinship, J. C., Berhe, A. A., Crow, S. E., Druhan, J. L., Heckman, K. A., Keiluweit, M.,
529 Lawrence, C. R., Marín-Spiotta, E., Plante, A. F., Rasmussen, C., Schädel, C., Schimel, J. P.,
530 Sierra, C. A., Thompson, A., Wagai, R., and Wieder, W. R.: Improving understanding of soil
531 organic matter dynamics by triangulating theories, measurements, and models,
532 *Biogeochemistry*, 140, 1–13, <https://doi.org/10.1007/s10533-018-0478-2>, 2018.

533 Bradford, M. A., Wood, S. A., Addicott, E. T., Fenichel, E. P., Fields, N., González-Rivero, J.,
534 Jevon, F. V., Maynard, D. S., Oldfield, E. E., Polussa, A., Ward, E. B., and Wieder, W. R.:
535 Quantifying microbial control of soil organic matter dynamics at macrosystem scales,
536 *Biogeochemistry*, <https://doi.org/10.1007/s10533-021-00789-5>, 2021.

537 Buchkowski, R. W., Bradford, M. A., Grandy, A. S., Schmitz, O. J., and Wieder, W. R.: Applying
538 population and community ecology theory to advance understanding of belowground
539 biogeochemistry, 20, 231–245, <https://doi.org/10.1111/ele.12712>, 2017.

540 Chakrawal, A., Herrmann, A. M., Koestel, J., Jarsjö, J., Nunan, N., Kätterer, T., and Manzoni, S.:
541 Dynamic upscaling of decomposition kinetics for carbon cycling models, 13, 1399–1429,
542 <https://doi.org/10.5194/gmd-13-1399-2020>, 2020.

543 Chesson, P.: Spatial scales in the study of reef fishes: A theoretical perspective, 23, 209–215,
544 <https://doi.org/10.1111/j.1442-9993.1998.tb00722.x>, 1998.

545 Chesson, P.: Scale transition theory with special reference to species coexistence in a
546 variable environment, 3, 149–163, <https://doi.org/10.1080/17513750802585491>, 2009.

547 Chesson, P.: Scale transition theory: Its aims, motivations and predictions, *Ecological*
548 *Complexity*, 10, 52–68, <https://doi.org/10.1016/j.ecocom.2011.11.002>, 2012.

549 Georgiou, K., Abramoff, R. Z., Harte, J., Riley, W. J., and Torn, M. S.: Microbial community-
550 level regulation explains soil carbon responses to long-term litter manipulations, 8, 1223,
551 <https://doi.org/10.1038/s41467-017-01116-z>, 2017.

552 Gomez-Casanovas, N., DeLucia, N. J., Bernacchi, C. J., Boughton, E. H., Sparks, J. P.,
553 Chamberlain, S. D., and DeLucia, E. H.: Grazing alters net ecosystem C fluxes and the global
554 warming potential of a subtropical pasture, 28, 557–572,
555 <https://doi.org/10.1002/eap.1670>, 2018.

556 Lehmann, J., Hansel, C. M., Kaiser, C., Kleber, M., Maher, K., Manzoni, S., Nunan, N.,
557 Reichstein, M., Schimel, J. P., Torn, M. S., Wieder, W. R., and Kögel-Knabner, I.: Persistence of
558 soil organic carbon caused by functional complexity, 13, 529–534,
559 <https://doi.org/10.1038/s41561-020-0612-3>, 2020.

560 Levin, S. A.: The problem of pattern and scale in Ecology: the Robert H. MacArthur award
561 lecture, *Ecology*, 73, 1943–1967, <https://doi.org/10.2307/1941447>, 1992.

562 Linn, D. M. and Doran, J. W.: Effect of Water-Filled Pore Space on Carbon Dioxide and
563 Nitrous Oxide Production in Tilled and Nontilled Soils, 48, 1267–1272,
564 <https://doi.org/10.2136/sssaj1984.03615995004800060013x>, 1984.

565 Parton, W. J., Schimel, D. S., Cole, C. V., and Ojima, D. S.: Analysis of factors controlling soil
566 organic matter levels in Great Plains grasslands, 51, 1173,
567 <https://doi.org/10.2136/sssaj1987.03615995005100050015x>, 1987.

568 Ross, S.: A first course in probability, Pearson Education India, 2002.

569 Schmidt, M. W. I., Torn, M. S., Abiven, S., Dittmar, T., Guggenberger, G., Janssens, I. A., Kleber,
570 M., Kögel-Knabner, I., Lehmann, J., Manning, D. A. C., Nannipieri, P., Rasse, D. P., Weiner, S.,
571 and Trumbore, S. E.: Persistence of soil organic matter as an ecosystem property, *Nature*,
572 478, 49–56, <https://doi.org/10.1038/nature10386>, 2011.

573 Sihi, D., Gerber, S., Inglett, P. W., and Inglett, K. S.: Comparing models of microbial–substrate
574 interactions and their response to warming, *Biogeosciences*, 13, 1733–1752,
575 <https://doi.org/10.5194/bg-13-1733-2016>, 2016.

576 Tang, J. and Riley, W. J.: A Theory of Effective Microbial Substrate Affinity Parameters in
577 Variably Saturated Soils and an Example Application to Aerobic Soil Heterotrophic
578 Respiration, 124, 918–940, <https://doi.org/10.1029/2018JG004779>, 2019.

579 Todd-Brown, K. E. O., Zheng, B., and Crowther, T. W.: Field-warmed soil carbon changes
580 imply high 21st-century modeling uncertainty, 15, 3659–3671,
581 <https://doi.org/10.3929/ethz-b-000272804>, 2018.

582 Van Oijen, M., Cameron, D., Levy, P. E., and Preston, R.: Correcting errors from spatial
583 upscaling of nonlinear greenhouse gas flux models, *Environmental Modelling & Software*,
584 94, 157–165, <https://doi.org/10.1016/j.envsoft.2017.03.023>, 2017.

585 Wang, Y. P., Chen, B. C., Wieder, W. R., Leite, M., Medlyn, B. E., Rasmussen, M., Smith, M. J.,
586 Augusto, F. B., Hoffman, F., and Luo, Y. Q.: Oscillatory behavior of two nonlinear microbial
587 models of soil carbon decomposition, 11, 1817–1831, <https://doi.org/10.5194/bg-11-1817-2014>, 2014.

589 Wieder, W. R., Bonan, G. B., and Allison, S. D.: Global soil carbon projections are improved
590 by modelling microbial processes, *Nature Clim. Change*, 3, 909–912,
591 <https://doi.org/10.1038/nclimate1951>, 2013.

592 Wieder, W. R., Allison, S. D., Davidson, E. A., Georgiou, K., Hararuk, O., He, Y., Hopkins, F.,
593 Luo, Y., Smith, M. J., Sulman, B., Todd-Brown, K., Wang, Y.-P., Xia, J., and Xu, X.: Explicitly
594 representing soil microbial processes in Earth system models, *Global Biogeochem. Cycles*,
595 29, 2015GB005188, <https://doi.org/10.1002/2015GB005188>, 2015.

596 Yan, Z., Bond-Lamberty, B., Todd-Brown, K. E., Bailey, V. L., Li, S., Liu, C., and Liu, C.: A
597 moisture function of soil heterotrophic respiration that incorporates microscale processes,
598 9, 2562, <https://doi.org/10.1038/s41467-018-04971-6>, 2018.

599 Yao, Y., Vehtari, A., Simpson, D., and Gelman, A.: Using stacking to average bayesian
600 predictive distributions, *Bayesian Anal.*, <https://doi.org/10.1214/17-BA1091>, 2018.

601